Partial CSI Acquisition for Size-Constrained Massive MIMO Systems With User Mobility

Jun Qian, Christos Masouros, *Senior Member, IEEE*, and Adrian Garcia-Rodriguez, *Member, IEEE*

***Abstract*—We propose a low-complexity approach for the downlink of physically constrained massive multiple-input multiple-output (MIMO) systems with user mobility. We examine a channel state information (CSI) acquisition strategy that exploits both the spatial and temporal correlations among the channels of adjacent base station antennas. The proposed strategy solely collects CSI for a subset of antennas and time frames. Then full CSI is approximated using the CSI of adjacent antennas and previous frames. This critically reduces the CSI acquisition complexity while sacrificing the CSI quality and, hence, introduces a scalable performance-complexity tradeoff. The numerical results demonstrate that, for practical mobile speeds, the proposed scheme reduces the computational complexity and enhances the energy efficiency of massive MIMO base stations against systems with complete CSI, while approximately preserving performance.**

***Index Terms*—Massive MIMO, partial CSI, temporal and spatial correlations, energy efficiency.**

I. Introduction

Massive multiple-input multiple-output (MIMO) has received great attention thanks to its potential to address the increasing data rate demands via serving a significant number of users simultaneously [1]. While massive MIMO promotes the use of linear precoding techniques such as zero forcing, the colossal number of antennas still imposes significant computational complexity requirements [2], [3]. Moreover, since these techniques rely on the availability of instantaneous CSI, a number of channel estimation schemes have been developed to enhance its acquisition [1], [3], [4].

When employing large antenna arrays in confined physical spaces with user mobility, both spatial and temporal correlations become determinant for the resulting performance. Recent studies have shown that these correlations can in fact be exploited. For instance, temporal channel correlation and the detected data symbols can be leveraged in time division duplex (TDD) massive MIMO systems to address pilot contamination [5], while the correlation between antennas is employed to optimize the CSI acquisition stage in frequency division duplex (FDD) systems [6]. The effect of nonisotropic scattering and user mobility on channel capacity is studied in [7]. Measured results with moderate user mobility in a LOS scenario are presented in [8]. Most relevant to this work, space-constrained antenna deployments are studied in [9], [10]. Similarly, low-complexity strategies to preserve the performance of space-limited massive MIMO are presented in [11]–[13].

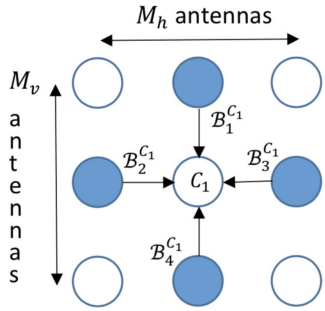

Fig. 1. Example CSI distribution pattern for a URA with $N_t = 9$, $N_c = 4$. Colored and white elements represent antennas with and without CSI acquisition, respectively.

This paper proposes to exploit temporal and spatial correlation jointly for size-constrained massive MIMO base stations (BSs). Specifically, instantaneous CSI is acquired for a subset of BS antennas and time frames. For those antennas without CSI, channel estimates are obtained by exploiting spatial correlation among adjacent antennas. For those frames without an explicit CSI acquisition phase, the channel coefficients are estimated from the CSI previously available by exploiting the channel's temporal correlation related to user mobility. This therefore extends the results of [11] where only spatial correlation is exploited in scenarios without user mobility. Our strategy leads to reduced complexity for CSI acquisition, at the expense of CSI quality and the resulting performance. Accordingly, we study the channel estimation error introduced by the proposed approach with respect to the perfect and frequent CSI acquisition. Our analysis and simulations show an overall favourable trade-off for the proposed strategy with partial CSI.

II. System Model and Partial CSI Acquisition

A. Physically Constrained Channel Model

Consider a general massive MIMO system with N_t antennas at the BS and N_r single-antenna users ($N_t \geq N_r$). The BS antennas are arranged in a uniform rectangular array (URA) topology. As shown in Fig. 1, M_h and M_v denote the number of antennas deployed horizontally and vertically respectively with $N_t = M_h \times M_v$. The signal received during downlink transmission at the k-th user is given by [11]

$$\mathrm{y}_k = \sqrt{\rho_\mathrm{f}}\mathbf{h}_k \mathbf{x} + n_k, \tag{1}$$

where $\mathbf{x} \in \mathbb{C}^{N_t \times 1}$ represents the transmitted symbols from the BS, $\mathbf{h}_k \in \mathbb{C}^{1\times N_t}$ denotes the k-th column of the downlink communication channel matrix $\mathbf{H} \in \mathbb{C}^{N_r \times N_t}$ from the BS to the k-th user, ρ_f denotes the SNR, and $n_k \sim \mathcal{CN}(0,\ 1)$ is the standard additive white Gaussian noise. The transmit signal can be further decomposed as $\mathbf{x} = w \cdot \mathbf{F}\mathbf{s}$, where $\mathbf{s} \in \mathbb{C}^{N_r \times 1}$ denotes the conveyed user symbols, $\mathbf{F} \in \mathbb{C}^{N_t \times N_r}$ represents a linear precoding matrix, and $w = 1/\sqrt{\{\mathrm{Tr}[\mathbf{F}\mathbf{F}^\mathrm{H}]\}}$ is a normalization constant guaranteeing the average transmission power $P_t = \mathbb{E}\{\mathbf{x}^\mathrm{H}\mathbf{x}\} = 1$. In the following we concentrate on zero-forcing (ZF) precoding for which

$$\mathbf{F} = \widetilde{\mathbf{H}}^\mathrm{H}(\widetilde{\mathbf{H}}\widetilde{\mathbf{H}}^\mathrm{H})^{-1}, \tag{2}$$

Manuscript received December 16, 2017; revised April 21, 2018; accepted June 1, 2018. Date of publication June 20, 2018; date of current version September 17, 2018. This work was supported by the Engineering and Physical Sciences Research Council project EP/M014150/1. The review of this paper was coordinated by Prof. H.-F. Lu. *(Corresponding author: Jun Qian.)*

J. Qian and C. Masouros are with the Department of Electronic and Electrical Engineering, University College London, London WC1E 7JE, U.K. (e-mail: jun.qian.15@ucl.ac.uk; c.masouros@ucl.ac.uk).

A. Garcia-Rodriguez was with the University College London, London WC1E 7JE U.K. He is now with Nokia Bell Labs, Dublin, Dublin 15, Ireland (e-mail: adrian.garcia_rodriguez@nokia-bell-labs.com).

Color versions of one or more of the figures in this paper are available online at http://ieeexplore.ieee.org.

Digital Object Identifier 10.1109/TVT.2018.2849263

where $\widetilde{\mathbf{H}}$ represents the downlink channel estimate. In this paper, we consider that the BS has to be deployed in a confined physical space and assume an impedance matching network that resolves any mutual coupling effects at the transmitter [14]. Thus, the downlink propagation channel to k-th user is modeled as [9], [15]

$$\mathbf{h}_k = \mathbf{g}_k \mathbf{A}_k, \tag{3}$$

where $\mathbf{g}_k \sim \mathcal{CN}(0, \mathbf{I}_{D_k})$, D_k denotes the number of signal propagation paths with different angles of departure, and $\mathbf{A}_k \in \mathbb{C}^{D_k \times N_t}$ is the transmit steering matrix of the k-th user given by [11], [12]

$$\mathbf{A}_k = \tfrac{1}{\sqrt{D_k}}[\mathbf{a}^{\mathrm{T}}(\theta_{k,1}, \phi_{k,1}), \ldots, \mathbf{a}^{\mathrm{T}}(\theta_{k,D_k}, \phi_{k,D_k})]^{\mathrm{T}}. \tag{4}$$

Here, $\theta_{k,i}$ and $\phi_{k,i}$ represent the azimuth and elevation angles describing the directions of departure respectively. The steering vectors $\mathbf{a}$ for the URA topology adopt the form [10], [16]

$$\mathbf{a}(\theta_{k,i}, \phi_{k,i}) = \big[1, e^{j2\pi[d_h \sin(\phi_{k,i})\sin(\theta_{k,i})]}, \ldots, e^{j2\pi[(M_h-1)d_h \sin(\phi_{k,i})\sin(\theta_{k,i})+(M_v-1)d_v \sin(\phi_{k,i})\cos(\theta_{k,i})]}\big], \tag{5}$$

where d_h and d_v represent the horizontal and vertical inter-antenna spacing normalized by the carrier wavelength λ respectively. Note that, receive correlation is not considered, since the inter-user spacing is significantly greater than λ [12].

We further consider a model accounting for the temporal correlation among the channels of adjacent frames with user mobility. Let l represent the index of the frame sample with CSI collection. In the following we adopt the autoregressive model AR(1) for temporal correlation studied in [17]. The actual channel for the $(l+1)$-th frame without pilot training stage for CSI acquisition can be expressed as [17], [18]

$$\mathbf{H}_{l+1} = \rho \mathbf{H}_l + \sqrt{1-\rho^2} \cdot \mathbf{E}, \tag{6}$$

where ρ represents the correlation coefficient computed by the zeroth-order Bessel function of the first kind $\rho = J_0(2\pi f_d \tau)$ with Doppler spread $f_d = f_c \frac{v}{c}$. Here, f_c is the carrier frequency, v is the user speed and c is the speed of light [17], [19]. Moreover, the rows of $\mathbf{E} \in \mathbb{C}^{N_r \times N_t}$ is expressed as $\mathbf{e}_k = \mathbf{z}_k \mathbf{A}_k$, where $\mathbf{z}_k \sim \mathcal{CN}(0, \mathbf{I}_{D_k})$ is uncorrelated with $\mathbf{g}_k$ [17].

B. Distribution of the CSI Acquisition

The presence of temporal correlation between transmitted frames for low and moderate user velocities motivates us to consider the probability of collecting CSI for only a subset of frames. We employ antenna activation pattern such as the one studied in detail in [11] to distribute the CSI. We only consider an elementary example, as shown in Fig. 1 for a model with 3×3 URA. Here, the $N_c = 4$ active antennas are denoted by the shaded elements.

More generally, in this paper, we study a model comprised of N_{total} frames. In this system, CSI is acquired in a subset $N_a \leq N_{\text{total}}$ of these frames and solely for a reduced number $N_c \leq N_t$ of antennas. The CSI distribution pattern in Fig. 1 is employed for N_a frames with CSI. To avoid repetition, we refer the reader to [11] for a more systematic study of the antenna activation patterns in the general case.

Let $\mathcal{B}$ and $\mathcal{C}$ denote the subsets of indices for active and inactive antennas during the CSI acquisition stage respectively [11]. The channel estimate for active antennas in $\mathcal{B}$ is

$$\widetilde{\mathbf{h}}_k|_{[\mathcal{B}]} = \left(\sqrt{1-\tau_k^2}\mathbf{h}_k + \tau_k \mathbf{q}_k \mathbf{A}_k\right)\Big|_{[\mathcal{B}]}, \tag{7}$$

Algorithm 1: Pseudocode of the frame distribution algorithm.

Inputs: N_{total}, N_a;
Output: $N_{\text{active}}, \widetilde{\mathbf{H}}_l$
$N_{\text{active}} = \text{zeros}(1, N_{\text{total}})$ (Initialization)
$\lceil N_{\text{total}}/N_a \rceil = N_g \leftarrow$ {The largest interval between adjacent frames with CSI acqusition, which are equally spaced }
{***First stage***: The distribution of the first $N_a \leq 0.5N_{\text{total}}$ frames where CSI is acquired }
For $i = 1 : N_g : N_{\text{total}}$ **do**
  $N_{\text{active}}(1, i) = 1 \leftarrow$ {To equally space the frames to acquire CSI from the first transmitted frame}
end for
{ ***Second stage***: When $N_a > 0.5N_{\text{total}}$, the distribution of the rest $(N_a - \lceil 0.5N_{\text{total}} \rceil)$ frames where CSI is acquired }
If $N_a > 0.5N_{\text{total}}$ **then**
  $a = 2 : N_g : N_{\text{total}}$;
  for $j = 1 \rightarrow (N_a - \lceil N_{\text{total}}/N_g \rceil)$ **do**
    $N_{\text{active}}(1, a(j)) = 1 \leftarrow$ { To equally space the rest $(N_a - \lceil 0.5N_{\text{total}} \rceil)$ frames with CSI acquisition }
  end for
end if
{ 15 – 21: The channel estimate for each frame }
for $l = 1 \rightarrow N_{\text{total}}$ **do**
  if $N_{\text{active}}(1, l) == 1$ **then**
    $\widetilde{\mathbf{H}}_l \leftarrow$ {Channel estimate following Eq.(7) – (8)}
  else
    $\widetilde{\mathbf{H}}_l = \widetilde{\mathbf{H}}_{l-1}$;
  end if
end for

where $\tau_k \in [0,1]$ models the quality of acquired CSI, $\mathbf{q}_k \sim \mathcal{CN}(0, \mathbf{I}_{D_k})$ is uncorrelated with $\mathbf{g}_k$ [9], [11]. The CSI of inactive antennas in $\mathcal{C}$ is obtained by averaging the CSI of adjacent active antennas

$$\widetilde{\mathbf{h}}_{k,\mathcal{C}_n} = \tfrac{1}{M_{\mathcal{C}_n}} \textstyle\sum_{i \in M_{\mathcal{C}_n}} \widetilde{\mathbf{h}}_{k,B_i^{\mathcal{C}_n}}. \tag{8}$$

where $M_{\mathcal{C}_n}$ represents the number of antennas with available CSI that are used to approximate the CSI of a specific antenna $\mathcal{C}_n$. Intuitively, the CSI of the $\mathcal{C}_n$-th antenna is computed through an average of the CSI from its closest antennas, $B_i^{\mathcal{C}_n}$. An example of the distribution is shown in Fig. 1. This approach has been selected for its low computational complexity, as analyzed in Sec. III-B. Note that (7)–(8) are used to estimate the channel during N_a frames with CSI, while the channel estimates of other frames are obtained by using the previous CSI. For completeness, the pseudocode of the frame distribution algorithm with the computation of estimated channels following (7)–(8) is presented in Algorithm 1.

III. System Performance Analysis

A. Channel Estimation Error Under Partial CSI

We concentrate on the channel estimation error introduced by the proposed strategy in this section. The channel estimation error $\widehat{\mathbf{h}}_k$ for the k-th user in a frame duration is given by

$$\widehat{\mathbf{h}}_k = \mathbf{h}_k - \widetilde{\mathbf{h}}_k, \tag{9}$$

In the following we use the mean square error (MSE) to calculate the channel estimation error factor of the l-th frame, which is given

$$\delta_k^{l+m} = \frac{1}{\sum_{n=1}^{N_t}\left[\rho^{2(l+m-1)} + \left(\frac{(1-\rho^{l+m-1})\sqrt{1-\rho^2}}{1-\rho}\right)^2\right]\Theta_k|_{[n,n]}}$$
$$\times\left\{\sum_{n\in\mathcal{B}}\left[\left(\rho^{l-1}\left(\rho^m-\sqrt{1-\tau_k^2}\right)\right)^2+\left(\frac{\left[(1-\rho^{l+m-1})-(1-\rho^{l-1})\sqrt{1-\tau_k^2}\right]\sqrt{1-\rho^2}}{1-\rho}\right)^2+\tau_k^2\right]\Theta_k|_{[n,n]}\right.$$
$$+\sum_{n\in\mathcal{C}}\left[\left(\rho^{2(l+m-1)}+\left(\frac{(1-\rho^{l+m-1})\sqrt{1-\rho^2}}{1-\rho}\right)^2\right)\Theta_k|_{[n,n]}\right.$$
$$+\frac{1}{M_n^2}\sum_{i\in\mathcal{B}^n}\left[\left(\rho^{l-1}\sqrt{1-\tau_k^2}\right)^2+\left(\frac{\left(1-\rho^{l-1}\right)\sqrt{1-\rho^2}\sqrt{1-\tau_k^2}}{1-\rho}\right)^2+\tau_k^2\right]\Theta_k|_{[i,i]}$$
$$-\frac{2\sqrt{1-\tau_k^2}}{M_n}\,\mathrm{Re}\left(\sum_{i\in\mathcal{B}^n}\left[\rho^{2l+m-2}+\frac{(1-\rho^{l+m-1})(1-\rho^{l-1})(1-\rho^2)}{(1-\rho)^2}\right]\Theta_k|_{[n,i]}\right)$$
$$\left.\left.+\frac{2}{M_n^2}\,\mathrm{Re}\left(\sum_{i,j\in\mathcal{B}^n,i>j}\left[\left(\rho^{l-1}\sqrt{1-\tau_k^2}\right)^2+\left(\frac{(1-\rho^{l-1})\sqrt{1-\rho^2}\sqrt{1-\tau_k^2}}{1-\rho}\right)^2+\tau_k^2\right]\Theta_k|_{[j,i]}\right)\right]\right\} \quad (14)$$

by [11]

$$\delta_k^l = \frac{\mathbb{E}\left\{\|\widehat{\mathbf{h}}_k\|_2^2\right\}}{\mathbb{E}\left\{\|\mathbf{h}_k\|_2^2\right\}} = \frac{\mathbb{E}\left\{\|\mathbf{h}_k-\widetilde{\mathbf{h}}_k\|_2^2\right\}}{\mathbb{E}\left\{\|\mathbf{h}_k\|_2^2\right\}}, \quad (10)$$

According to Sec. II, the distribution of frames with CSI acquisition are defined by Algorithm 1. If the index of the frame with CSI is l, the indices of following frames without CSI can be $[l+1, l+2, \ldots, l+m]$. In view of the analysis in [11], in this paper, the channel estimation error factor generated by the proposed strategy with temporal correlation for the k-th user in the $(l+m)$-th frame is defined in the following. First, δ_k^{l+m} following (10) can be decomposed as

$$\delta_k^{l+m} = \frac{\mathbb{E}\left\{\sum_{n\in\mathcal{B}}|\widehat{\mathrm{h}}_{k,n}^{l+m}|^2+\sum_{n\in\mathcal{C}}|\widehat{\mathrm{h}}_{k,n}^{l+m}|^2\right\}}{\mathbb{E}\left\{\sum_{N_t}|\mathrm{h}_{k,n}^{l+m}|^2\right\}}, \quad (11)$$

where $\widehat{\mathrm{h}}_{k,n}^{l+m}$ is the channel estimation error from the n-th BS antenna to the k-th user in the $(l+m)$-th frame. Following the physical channel model defined in (3), we have $\mathbb{E}\left\{\sum_{N_t}|\mathrm{h}_{k,n}|^2\right\} = N_t$ and $\mathbb{E}\left\{|\widehat{\mathrm{h}}_{k,n}|^2\right\} = \mathrm{var}\left(\widehat{\mathrm{h}}_{k,n}\right)$. Therefore, in (11), the factors in the first part involving the subset $\mathcal{B}$ of active antennas in the l-th frame referring to (6) can be expressed as

$$\mathbb{E}\left\{|\widehat{\mathrm{h}}_{k,n}^{l+m}|^2\right\} = \mathbb{E}\left\{|\mathrm{h}_{k,n}^{l+m}-\widetilde{\mathrm{h}}_{k,n}^{l+m}|^2\right\}$$
$$=\mathbb{E}\left\{\left|\rho^{l+m-1}\mathrm{h}_{k,n}+\frac{(1-\rho^{l+m-1})\sqrt{1-\rho^2}}{1-\rho}\mathrm{e}_{k,n}\right.\right.$$
$$-\rho^{l-1}\sqrt{1-\tau_k^2}\cdot\mathrm{h}_{k,n}-\frac{(1-\rho^{l-1})\sqrt{1-\rho^2}\sqrt{1-\tau_k^2}}{1-\rho}$$
$$\left.\left.\times\,\mathrm{e}_{k,n}-\tau_k\mathbf{q}_k\mathbf{A}_k|_{[n]}\right|^2\right\}, n\in\mathcal{B}, \quad (12)$$

Here, $e_{k,n} = \mathbf{z}_k\mathbf{A}_k|_{[n]}$, where $\mathbf{z}_k\mathbf{A}_k$ represents the vectors of $\mathbf{E}$ defined in Sec. II-A. The computation of $\widetilde{\mathrm{h}}_{k,n}|_{[\mathcal{B}]}$ for active antennas in the l-th frame follows (7). For the second part with the subset $\mathcal{C}$ of inactive antennas in (11), the factors introduced by averaging approach and partial channel estimate can be computed as

$$\mathrm{var}\left(\widehat{\mathrm{h}}_{k,n}^{l+m}\right) = \mathrm{var}\left(\mathrm{h}_{k,n}^{l+m}-\frac{1}{M_n}\sum_{i=1}^{M_n}\widetilde{\mathrm{h}}_{k,\mathcal{B}_i^n}^{l+m}\right)$$
$$=\mathrm{var}\left(\rho^{l+m-1}\mathrm{h}_{k,n}+\frac{(1-\rho^{l+m-1})\sqrt{1-\rho^2}}{1-\rho}e_{k,n}\right.$$
$$-\frac{1}{M_n}\sum_{i=1}^{M_n}\left[\rho^{l-1}\sqrt{1-\tau_k^2}\cdot\mathrm{h}_{k,\mathcal{B}_i^n}\right.$$
$$+\frac{(1-\rho^{l-1})\sqrt{1-\rho^2}\sqrt{1-\tau_k^2}}{1-\rho}\mathrm{e}_{k,\mathcal{B}_i^n}$$
$$\left.\left.+\tau_k\mathbf{q}_k\mathbf{A}_k|_{[\mathcal{B}_i^n]}\right]\right), n\in\mathcal{C}, \quad (13)$$

where $\frac{1}{M_n}\sum_{i=1}^{M_n}\widetilde{\mathrm{h}}_{k,\mathcal{B}_i^n}$ computes the channel estimate for inactive antennas in l-th frame with CSI following (7)–(8). Based on the above expression, the channel estimation error factor for $(l+m)$-th frame can be given (14) shown at the top of the page.

In (14), $\Theta_k = \mathbb{E}\left\{\mathbf{h}_k^{\mathrm{H}}\mathbf{h}_k\right\} = \mathbf{A}_k^{\mathrm{H}}\mathbf{A}_k$ is the channel correlation matrix of k-th user. Meanwhile, $\mathcal{B}^n$ and M_n denote the indices and the number of adjacent antennas for CSI computation of n-th antenna respectively. m can be considered as the index of frame without CSI when l-th frame with CSI is set to be initial. When $m=0$, channel estimation error factor for the l-th frame with CSI acquisition can be obtained. In the proposed N_{total}-frame model, each frame has its own δ_k^l for k-th

TABLE I
COMPUTATIONAL COMPLEXITY (FLOPS) AT THE BASE STATION

Communication Phase	*Complexity in flops*
CSI acquisition phase (only for N_a frames)	$C^{\text{tr}} = 8N_cN_r\eta_{\text{tr}} = 8N_cN_r^2$
Downlink phase	$C^{\text{d}} = C^{\text{d}}_{\text{inv}} + C^{\text{d}}_{\text{d}}$
· Signal generation	$C^{\text{d}}_{\text{d}} = 8N_cN_r\eta_{\text{dl}}$
· Precoding matrix	$C^{\text{d}}_{\text{inv}} = \left(24N_r^3 + 16N_r^2N_t\right) + N_r + \left(2N_rN_t + 8N_r^2N_t\right)$
Uplink phase	$C^{\text{u}} = 8N_tN_r\eta_{\text{ul}}$

user; therefore, the average channel estimation error factor for k-th user is computed as $\overline{\delta}_k = \frac{1}{N_{\text{total}}}\sum_{l=1}^{N_{\text{total}}}\delta_k^l$.

B. Complexity Analysis

In this section, the signal processing complexity of the proposed strategy is studied. The global complexity is computed based on the three phases of TDD communication system[1] including CSI acquisition, downlink transmission and uplink reception following the analysis in [2], [11].

The complexity for each phase is shown in Table I [2], [11], where η_{tr}, η_{dl} and η_{ul} represent the time resources allocated to each phase respectively. The process of generating the channel estimate from the received pilot signals determines the complexity C^{tr} during the CSI acquisition stage [2]. The downlink stage comprising the precoding matrix and transmit signals generator results in the complexity $C^{\text{d}} = C^{\text{d}}_{\text{inv}} + C^{\text{d}}_{\text{d}}$. Here, $C^{\text{d}}_{\text{inv}}$ accounts for computing the ZF precoding matrix, whereas C^{d}_{d} accounts for computing precoded signals obtained via the strategy studied in [2], [11]. In TDD systems, the uplink detection matrix can be obtained at no cost due to channel reciprocity, and C^{u} stands for the operations related to data reception [11].

For the proposed temporally-spatially correlated channel model, only N_a frames perform the pilot correlation process during the CSI acquisition stage. The remaining frames only implement data transmission and reception using previous CSI. Therefore, the complexity for frames where CSI is acquired can be expressed as

$$C^A_{\text{total}} = C^{\text{tr}} + C^{\text{d}} + C^{\text{u}}. \tag{15}$$

Instead, for the rest of the frames we have

$$C^I_{\text{total}} = C^{\text{d}} + C^{\text{u}}. \tag{16}$$

Accordingly, the average total complexity per frame in the N_{total}-frame model can be expressed as

$$\overline{C}_{\text{total}} = \frac{1}{N_{\text{total}}}\left[N_a \cdot C^A_{\text{total}} + (N_{\text{total}} - N_a) \cdot C^I_{\text{total}}\right]. \tag{17}$$

C. Achievable Ergodic Rates and Energy Efficiency

In this section, the effects of partial CSI acquisition on the ergodic sum rate (spectral efficiency) and energy efficiency of the massive MIMO system are studied.

1) Ergodic Downlink Sum Rates: The downlink ergodic sum rates of the communication system for the l-th frame can be defined as

$$\text{R}^l_{\text{sum}} = \eta_{\text{dl}}/\eta_{\text{coh}} \cdot B\sum_{k=1}^{K}\log_2(1+\gamma_k^l), \tag{18}$$

where η_{coh} is the number of coherence symbols of the channel, and $\eta_{\text{dl}}/\eta_{\text{coh}}$ represents the proportion of the time allocated to downlink transmission. B denotes the system bandwidth, and $S_k^l = \log_2(1+\gamma_k^l)$ refers to the spectral efficiency of k-th user in l-th frame. Moreover, γ_k^l stands for the associated SINR [11]

$$\gamma_k^l = \frac{w^2|\,\mathbb{E}\left\{\mathbf{h}_k^{\text{H}}\mathbf{f}_k\right\}|^2}{\frac{1}{\rho_{\text{f}}} + w^2\text{var}\left(\mathbf{h}_k^{\text{H}}\mathbf{f}_k\right) + w^2\sum_{i\neq k}\mathbb{E}\left\{|\mathbf{h}_k^{\text{H}}\mathbf{f}_i|^2\right\}}, \tag{19}$$

where $\mathbf{f}_k$ is the k-th column of the precoding matrix defined in Sec. II-A, which follows (2),(6)–(8) for the examined l-th frame. Moreover, for the proposed N_{total}-frame model, the average spectral efficiency achievable for each user in each frame can be computed as $\overline{S}_k = \frac{1}{N_{\text{total}}}\sum_{l=1}^{N_{\text{total}}}\{\frac{1}{N_r}\sum_{k=1}^{N_r}S_k^l\}$.

2) Energy Efficiency: The resulting energy efficiency for downlink transmission in the l-th frame is given as [20]

$$\epsilon_l = \frac{\text{R}^l_{\text{sum}}}{P_{\text{tot}}}, \tag{20}$$

where P_{tot} represents the total transmission power consumption and can be decomposed as [11], [20]

$$P_{\text{tot}} = \frac{P_{\text{PA}} + P_{\text{RF}} + P_{\text{BB}}}{(1-\sigma_{\text{DC}})(1-\sigma_{\text{MS}})(1-\sigma_{\text{cool}})}, \tag{21}$$

Here, $\sigma_{\text{DC}}, \sigma_{\text{MS}}$ and $\sigma_{\text{cool}} \in (0,1)$ denote the parameters characterizing DC-DC loss, power supplies loss and active cooling loss respectively. P_{PA} and P_{RF} represent the power consumed by power amplifiers and other electronic components in the RF chains respectively. $P_{\text{BB}} = p_cC$ denotes the power consumption of digital signal processor. Here, p_c denotes the power consumption per real flop and C corresponds to the number of real floating point operations per second determined by (15)-(16) for frames with and without CSI acquisition, respectively [11], [20]. Therefore, considering the computational complexity, the total transmission power consumption following (21) can be further given by

$$P_{\text{tot}} = \begin{cases} P^A_{\text{tot}} & \propto C^A_{\text{total}} \text{ for frames with CSI,} \\ P^I_{\text{tot}} & \propto C^I_{\text{total}} \text{ for frames without CSI.} \end{cases} \tag{22}$$

For the N_{total}-frame model, each frame displays different energy efficiency due to varying complexity and channel estimate. The resulting energy efficiency ϵ_l for the l-th frame can be re-expressed as

$$\epsilon_l = \begin{cases} \text{R}^l_{\text{sum}}/P^A_{\text{tot}}, & \text{if the } l\text{-th frame is with CSI,} \\ \text{R}^l_{\text{sum}}/P^I_{\text{tot}}, & \text{if the } l\text{-th frame is without CSI.} \end{cases} \tag{23}$$

Accordingly, the average energy efficiency per frame in the N_{total}-frame model can be obtained by $\overline{\epsilon} = \frac{1}{N_{\text{total}}}\sum_{l=1}^{N_{\text{total}}}\epsilon_l$.

IV. SIMULATION RESULTS

We compare our approach to full CSI based on numerical results, for a scenario with $N_t = 144$, $N_r = 12$, $D_k = 50$, and varying number of active antennas N_c [11]. The angle spread of the azimuth and elevation angles is fixed to be $\pi/5$ and π respectively. Imperfect CSI estimation is considered with $\tau_k = 0.1$, the inter-antenna spacing is fixed to $d_v = d_h = 0.3$ λ, and the total system bandwidth is $B = 20$ MHz. The standard LTE frame with a time duration of 10 ms containing 140 OFDM symbols in total ($\eta_{\text{coh}} = 140$) is considered, where 70% symbols are assigned to downlink transmission [11]. We assume that the channel matrix stays constant for the frame duration with the time interval $\tau = 1$ ms [17], and consider a carrier frequency of $f_c = 2.5$ GHz. The total number of LTE frames examined for the temporal correlated model is $N_{\text{total}} = 10$. We consider a femtocell scenario for defining the power consumption parameters in [11].

[1]While the proposed technique could also be applied to massive MIMO systems operating in FDD, in the following we focus on the more practical TDD systems [1].

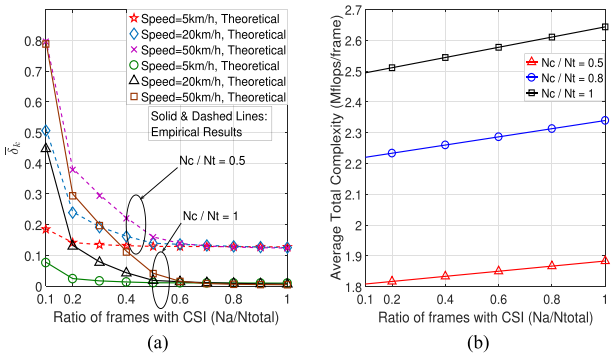

Fig. 2. Average (a) channel estimation error factor per user per frame $\overline{\delta}_k$ and (b) total complexity per frame with increasing N_a. $\eta_{\text{coh}} = 140$, $\eta_{\text{tr}} = N_r = 12$, $\eta_{\text{dl}} = 7 \times 14$ per frame. SNR $=$15 dB.

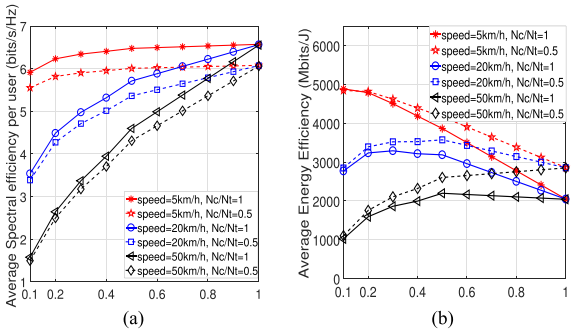

Fig. 3. Average (a) spectral efficiency per user per frame and (b) energy efficiency per frame with increasing N_a for a femtocell scenario and varying user velocity. SNR $=$ 15 dB.

The evolution of average channel estimation error factor per user per frame $\overline{\delta}_k$ for varying number of frames with CSI is shown in Fig. 2(a) for three scenarios with user velocities of 5, 20, and 50 km/h. The results of this figure corroborate the intuition that the channel estimation error factor increases with user mobility. Moreover, a close match between the theoretical error (markers) following (14) and the empirical error (solid and dashed lines) can be observed. Fig. 2(a) also shows that in most cases the channel estimation error becomes significant for $N_a/N_{\text{total}} \leq 1/2$ since CSI becomes highly outdated. The average total complexity per frame following (17) can be observed in Fig. 2(b), for increasing number N_a of frames with CSI. By employing the proposed approach, complexity savings can be further achieved when both spatial and temporal correlations are jointly exploited with smaller number of active antennas (N_c) and frames (N_a) dedicated to CSI acquisition.

The effect of N_a on the average spectral efficiency per user per frame is shown in Fig. 3(a). The results of this figure show that an increasing number of frames with CSI is required when the user velocity increases, which results in diminishing temporal correlation, to reach the performance obtained when $N_a = N_{\text{total}}$. Still, for low and moderate user velocities, close to optimal SE can be obtained with a reduced N_a. The benefits of acquiring CSI for a subset of time frames and antennas are further highlighted in Fig. 3(b), where the energy effciency is shown for increasing N_a. We note that the EE captures the trade-off between SE performance and complexity. Fig. 3(b) shows that reducing the number of frames with CSI can be beneficial to EE for low and moderate user velocities. Especially, when $v = 20$ km/h, the EE of the massive MIMO system considered can be maximized when $N_a \approx 0.5 N_{\text{total}}$, while even smaller N_a is optimal for lower mobility. Clearly, this occurs because the reduced power consumption in the RF chains compensates for the loss in the achievable data rates.

V. Conclusion

In this correspondence, we have proposed a CSI acquisition model making use of temporal and spatial correlations for size-constrained massive MIMO systems with user mobility. We exploit partial CSI acquisition and obtain significant complexity and power consumption gains. Our results demonstrate that the proposed scheme can achieve an energy efficiency enhancement while preserving the performance of size-constrained massive MIMO systems with complete CSI, especially for low and moderate user mobility scenarios.

References

[1] F. Rusek *et al.*, "Scaling up MIMO: Opportunities and challenges with very large arrays," *IEEE Sig. Process. Mag.*, vol. 30, no. 1, pp. 40–60, Jan. 2013.

[2] H. Yang and T. L. Marzetta, "Performance of conjugate and zero-forcing beamforming in large-scale antenna systems," *IEEE J. Sel. Areas Commun.*, vol. 31, no. 2, pp. 172–179, Feb. 2013.

[3] K. Zheng, L. Zhao, J. Mei, B. Shao, W. Xiang, and L. Hanzo, "Survey of large-scale MIMO systems," *IEEE Commun. Surveys Tut.*, vol. 17, no. 3, pp. 1738–1760, Jul./Sep. 2015.

[4] N. Shariati, E Bjrnson, M. Bengtsson, and M. Debbah, "Low-complexity polynomial channel estimation in large-scale MIMO with arbitrary statistics," *IEEE J. Sel. Topics Signal Process.*, vol. 8, no. 5, pp. 815–830, Oct. 2014.

[5] Y. Li, R. Wang, Y. Chen, and S. Zhu, "Exploiting temporal channel correlation in data-assisted massive MIMO uplink detection," *IEEE Commun. Lett.*, vol. 21, no. 2, pp. 430–433, Feb. 2017.

[6] B. Lee, J. Choi, J.-Y. Seol, D. J. Love, and B. Shim, "Antenna grouping based feedback compression for FDD-based massive MIMO systems," *IEEE Trans. Commun.*, vol. 63, no. 9, pp. 3261–3274, Sep. 2015.

[7] G. J. Byers and F. Takawira, "Spatially and temporally correlated MIMO channels: Modeling and capacity analysis," *IEEE Trans. Veh. Technol.*, vol. 53, no. 3, pp. 634–643, May 2004.

[8] P. Harris *et al.*, "Performance characterization of a real-time massive MIMO system with LOS mobile channels," *IEEE J. Sel. Areas Commun.*, vol. 35, no. 6, pp. 1244–1253, Jun. 2017.

[9] C. Masouros and M. Matthaiou, "Space-constrained massive MIMO: Hitting the wall of favorable propagation," *IEEE Commun. Lett.*, vol. 19, no. 5, pp. 771–774, May 2015.

[10] S. Biswas, C. Masouros, and T. Ratnarajah, "Performance analysis of large multiuser MIMO systems with space-constrained 2-D antenna arrays," *IEEE Trans. Wireless Commun.*, vol. 15, no. 5, pp. 3492–3505, May 2016.

[11] A. Garcia-Rodriguez and C. Masouros, "Exploiting the increasing correlation of space constrained massive MIMO for CSI relaxation," *IEEE Trans. Commun.*, vol. 64, no. 4, pp. 1572–1587, Apr. 2016.

[12] C. Masouros, M. Sellathurai, and T. Ratnarajah, "Large-scale MIMO transmitters in fixed physical spaces: The effect of transmit correlation and mutual coupling," *IEEE Trans. Commun.*, vol. 61, no. 7, pp. 2794–2804, Jul. 2013.

[13] H. Tataria, P. J. Smith, M. Matthaiou, and P. A. Dmochowski, "Uplink analysis of large MU-MIMO systems with space-constrained arrays in ricean fading," in *Proc. IEEE Int. Conf. Commun.*, May 2017, pp. 1–7.

[14] K. F. Warnick and M. A. Jensen, "Optimal noise matching for mutually coupled arrays," *IEEE Trans. Antennas Propag.*, vol. 55, no. 6, pp. 1726–1731, Jun. 2007.

[15] C. Wang and R. D. Murch, "Adaptive downlink multi-user MIMO wireless systems for correlated channels with imperfect CSI," *IEEE Trans. Wireless Commun.*, vol. 5, no. 9, pp. 2435–2446, Sep. 2006.

[16] D. Ying, F. W. Vook, T. A. Thomas, D. J. Love, and A. Ghosh, "Kronecker product correlation model and limited feedback codebook design in a 3D channel model," in *Proc. IEEE Int. Conf. Commun.*, Jun. 2014, pp. 5865–5870.

[17] K. T. Truong and R. W. Heath, "Effects of channel aging in massive MIMO systems," *J. Commun. Networks*, vol. 15, no. 4, pp. 338–351, Aug. 2013.

[18] R. H. Clarke, "A statistical theory of mobile-radio reception," *Bell Syst. Tech. J.*, vol. 47, no. 6, pp. 957–1000, Jul./Aug. 1968.

[19] J. Zhang, J. G. Andrews, and R. W. Heath, Jr., "Block diagonalization in the MIMO broadcast channel with delayed CSIT," in *Proc. IEEE Global Telecommun. Conf. GLOBECOM*, Nov. 2009, pp. 1–6.

[20] D. Ha, K. Lee, and J. Kang, "Energy efficiency analysis with circuit power consumption in massive MIMO systems," in *Proc. IEEE 24th Annu. Int. Symp. Pers., Indoor, Mobile Radio Commun*, Sep. 2013, pp. 938–942.